Analysis of A Predator-Prey Model with The Effects of Threshold Harvesting

La Ode Muhlis[1*] and *Amin* Mbusango[2]

[1]Department of Mathematics, Faculty of Mathematics and Natural Sciences, Papua University, 98312 Manokwari, Indonesia
[2]Department of Agriculture, Faculty of Agriculture, Papua University, 98312 Manokwari, Indonesia

Abstract. This study develops and analyzes a predator-prey model within an extended Lotka-Volterra framework that incorporates a Holling Type II functional response and a threshold-based harvesting strategy. Two ecological regimes were considered: a non-harvesting regime, where population densities remain below prescribed thresholds, and a harvesting regime activated once these thresholds are exceeded. The analysis begins with the identification of equilibrium points, followed by a local stability analysis using the Jacobian matrix and eigenvalue criteria. In the absence of harvesting, three biologically meaningful equilibria are obtained: trivial, semitrivial, and interior equilibria representing prey-predator coexistence. The stability of these equilibria depends on key biological parameters, such as predator mortality and prey intraspecific competition. When threshold harvesting is introduced, the interior equilibrium can be stabilized if the harvesting thresholds are chosen appropriately. Numerical simulations confirm that threshold-based harvesting may stabilize dynamics that are unstable in the non-harvesting case, although this effect is highly sensitive to harvesting parameters and exploitation intensity. The results highlight the importance of well-designed threshold harvesting policies for sustainable ecosystem management and long-term prey-predator coexistence.

1 Introduction

The predator-prey model, originally introduced by Lotka and Volterra, represents a classical mathematical framework based on a pair of differential equations that describe the interaction dynamics between two species, prey and predator. In this model, prey are organisms that are targeted for consumption by predators, whereas predators rely on prey as their primary resource for survival. Prey populations are assumed to grow exponentially in the absence of predators. Conversely, predators face extinction if the prey becomes unavailable. Thus, predators serve a dual role, not only influencing prey population dynamics, but also acting as natural regulators to prevent prey overpopulation. [2], in their seminal work, provides a comprehensive introduction to mathematical modeling in biology, including analyses and simulations that are essential for understanding population dynamics.

The predator-prey relationship remains a critical subject of study because of its significant implications for maintaining ecosystem balance, preserving biodiversity, and predicting the cascading effects of species loss within a food web. Disruptions in these interactions can destabilize ecosystems and spread throughout trophic structures [3]. Consequently, predator-prey dynamics continue to be a central focus of research in biology, ecology, and applied mathematics.

Over the years, the classical predator-prey model has been extended and refined to incorporate additional ecological complexities. For example, [7] explored predator-prey systems with role reversals and maturation delays, demonstrating the critical influence of such delays on population stability. Similarly, [4] analyzed the stochastic dynamics of the Leslie-Gower predator-prey model with feedback control and identified sufficient conditions for population persistence and extinction. [6] provided foundational insights into the stochastic properties of predator-prey models, emphasizing how variability and randomness influence species interactions and population stability. [5] examined the effects of prey migration oscillations on predator-prey dynamics, revealing that even minimal migration can facilitate coexistence between prey and predators.

Human activities, such as harvesting, also significantly affect population dynamics. Sustainable harvesting practices, particularly threshold harvesting, aim to ensure the long-term viability of populations by enforcing minimum thresholds. For instance, [9] investigated the effects of age structure in prey populations on threshold harvesting dynamics, revealing that maturation delays among immature prey substantially affect predator stability. [10] explored a predator-prey system within the Lotka-Volterra framework and found that threshold harvesting ceases when population levels fall below a defined threshold, thus ensuring sustainability. Furthermore, [8]

* Corresponding author: l.mukhlis@unipa.ac.id

demonstrated the uniqueness of limit cycles in cause-type predator-prey models, providing a rigorous mathematical foundation for understanding population oscillations and their ecological implications.

This study introduces a novel approach to the analysis of predator-prey interactions, distinguishing itself from prior research in two key respects. First, the model incorporates a Holling-Type II functional response, which realistically captures predator saturation under prey abundance conditions. Second, it examined the simultaneous effects of threshold harvesting on both prey and predator populations. This dual focus aims to advance our understanding of ecosystem-based population management and sustainable use of biological resources.

2 Materials and Methods

2.1 Model Formulation and Mathematical Framework

Predator–prey interactions constitute a fundamental class of ecological processes and have been the subject of extensive investigation in both theoretical and applied ecology. The mathematical modeling of predator–prey dynamics was originally introduced in the seminal works of Lotka and Volterra [1,11]. Despite its historical significance, the classical Lotka–Volterra model fails to account for ecological constraints, such as finite environmental resources, as it assumes unbounded population growth. This limitation reduces its applicability to real ecosystems, where population growth is inherently restricted by the environmental carrying capacity. Consequently, numerous extensions and modifications of the classical model have been proposed to achieve a more realistic description of predator–prey interactions.

In recent years, increasing attention has been paid to the incorporation of harvesting strategies into predator-prey models, particularly those based on threshold policies motivated by conservation and sustainable resource management. Threshold harvesting reflects regulatory practices in which harvesting is permitted only when population densities exceed the prescribed critical levels, thereby preventing overexploitation. Motivated by these considerations, this study developed a predator-prey model that integrates logistic prey growth, nonlinear predation, and threshold-based harvesting for both species.

To formulate the model, the following assumptions are adopted:

a. Let $x(t)$ and $y(t)$ denote the population densities of prey and predator, respectively, at time t.
b. In the absence of predators, the prey population grows logistically toward the environmental carrying capacity K with an intrinsic growth rate r.
c. The interaction between prey and predator populations is assumed to follow a Holling type II functional response, characterized by a half-saturation constant a and prey consumption rate n, capturing the saturation effect in predation at high prey densities.
d. In the absence of prey, the predator population declines at a rate proportional to the natural mortality rate d.
e. Parameter m represents the conversion efficiency of consumed prey biomass into predator population growth.
f. Furthermore, threshold harvesting was applied to both prey and predator populations to model regulated exploitation practices.

Based on these assumptions, predator-prey dynamics with threshold harvesting are governed by the following system of nonlinear differential equations:

$$\begin{aligned} \frac{dx}{dt} &= rx\left(1-\frac{x}{K}\right)-\frac{nxy}{a+x}-H(x), \\ \frac{dy}{dt} &= \frac{mnxy}{a+x}-dy-H(y), \end{aligned} \tag{1}$$

where $x \geq 0, y \geq 0$. Parameters a, d, K, m, n, and r are assumed to be positive constants. The threshold harvesting function is defined as follows:

$$\begin{aligned} H(x) &= \begin{cases} 0, & \text{if } x \leq T \\ \frac{p(x-T)}{p+(x-T)}, & \text{if } x > T \end{cases}, \\ H(y) &= \begin{cases} 0, & \text{if } y \leq R \\ \frac{q(y-R)}{q+(y-R)}, & \text{if } y > R \end{cases}, \end{aligned} \tag{2}$$

where T and R denote the harvesting threshold levels for the prey and predator populations, respectively, and p and q represent the corresponding maximum harvesting rates.

In system (1), harvesting is absent when the prey and predator population densities remain below their respective threshold levels, that is, when $x \leq T$ and $y \leq R$, leading to $H(x) = 0$ and $H(y) = 0$. Conversely, once the population densities exceed these thresholds, harvesting is activated and increases monotonically with the population size. As x and y increase relative to T and R, respectively, the harvesting rates asymptotically approach their corresponding maximum values, ensuring biologically realistic bounded harvesting intensities.

2.2 Model without Harvesting

In this subsection, we consider the predator-prey system in the absence of harvesting. Harvesting of both prey and predator populations is assumed to not occur when the population densities satisfy $x \leq T$ and $y \leq R$, respectively. This assumption reflects the conservation policies aimed at maintaining population sustainability. Under these conditions, the harvesting functions vanish, that is, $H(x) = 0$ and $H(y) = 0$. Consequently, system (1) reduces to the following predator–prey model without harvesting:

$$\begin{aligned} \frac{dx}{dt} &= rx\left(1-\frac{x}{K}\right)-\frac{nxy}{a+x}, \\ \frac{dy}{dt} &= \frac{mnxy}{a+x}-dy. \end{aligned} \tag{3}$$

To simplify the analysis and reduce the complexity arising from the presence of multiple parameters, a nondimensionalization of system (3) was performed. This procedure facilitates both qualitative and quantitative analyses by minimizing the number of independent parameters. Let the following dimensionless variables and parameters be introduced:

$$u(\tau) = \frac{x}{a}, \quad v(\tau) = \frac{ny}{ar}, \quad \sigma = \frac{a}{K},$$
$$\rho = \frac{mn}{r}, \quad \mu = \frac{d}{r}, \quad \tau = rt,$$

Substituting these transformations into system (3) yields the nondimensional system

$$\begin{aligned} \frac{du}{d\tau} &= u(1-\sigma u) - \frac{uv}{1+u}, \\ \frac{dv}{d\tau} &= \frac{\rho uv}{1+u} - \mu v, \end{aligned} \tag{4}$$

where σ, ρ, and μ are the positive dimensionless parameters. For convenience, we define $du/d\tau = f(u,v)$ and $dv/d\tau = g(u,v)$, where

$$f(u,v) = u(1-\sigma u) - \frac{uv}{1+u},$$
$$g(u,v) = \frac{\rho uv}{1+u} - \mu v.$$

The Jacobian matrix of system (4) evaluated at equilibrium point $E = (u^*, v^*)$ is given by

$$J_{E_{(u^*,v^*)}} = \begin{bmatrix} 1 - 2\sigma u^* - \frac{v^*}{(1+u^*)^2} & -\frac{u^*}{1+u^*} \\ \frac{\rho v^*}{(1+u^*)^2} & \frac{\rho u^*}{1+u^*} - \mu \end{bmatrix}. \tag{5}$$

By setting $du/d\tau = dv/d\tau = 0$, the equilibrium points of system (4) can be obtained. Provided that the conditions $\rho > \mu$ and $\rho > \mu(1+\sigma)$ hold, the system admits three equilibrium points in the first quadrant.

$E_0 = (0,0)$, $E_1 = \left(\frac{1}{\sigma}, 0\right)$, and $E_2 = \left(\frac{\mu}{\rho-\mu}, \frac{\rho^2 - \rho\mu(1+\sigma)}{(\rho-\mu)^2}\right)$.

To determine the local stability properties of each equilibrium point, a linear stability analysis was performed by evaluating the Jacobian matrix at the corresponding equilibrium and computing the eigenvalues from the characteristic equation:

$$\left| J_{E_{(u^*,v^*)}} - \lambda I \right| = 0$$

The nature of the resulting eigenvalues characterizes the stability behavior of the system in the neighborhood of each equilibrium point.

2.2.1 Stability Analysis of the Equilibrium Point E_0

The equilibrium point E_0 represents the trivial equilibrium, corresponding to the extinction of both prey and predator populations. The local stability of this equilibrium can be investigated by evaluating the Jacobian matrix given in Equation (5) at $E_0 = (0,0)$. Substituting $u^* = 0$ and $v^* = 0$ into (5) yields.

$$J_{E_0} = \begin{bmatrix} 1 & 0 \\ 0 & -\mu \end{bmatrix}.$$

The associated eigenvalues were $\lambda_1 = 1$ and $\lambda_2 = -\mu$. Because $\mu > 0$, it follows that one eigenvalue is positive, while the other is negative. Consequently, the equilibrium point E_0 is a saddle point, and is therefore unstable. This result indicates that the extinction state is unstable under small perturbations, implying that the system cannot persist in the vicinity of E_0.

2.2.2 Stability Analysis of the Equilibrium Point E_1

Equilibrium point E_1 is classified as a semi-trivial equilibrium, representing the persistence of the prey population in the absence of predators. Evaluating Jacobian matrix (5) at

$$E_1 = \left(\frac{1}{\sigma}, 0\right)$$

yields

$$J_{E_1} = \begin{bmatrix} -1 & -\frac{1}{1+\sigma} \\ 0 & \frac{\rho - \mu(1+\sigma)}{1+\sigma} \end{bmatrix}.$$

The eigenvalues of this matrix are

$$\lambda_1 = -1, \quad \lambda_2 = \frac{\rho - \mu(1+\sigma)}{1+\sigma}.$$

Because $\rho > \mu(1+\sigma)$, equilibrium point E_1 possesses one negative eigenvalue, λ_1, and one positive eigenvalue, λ_2, and is therefore classified as a saddle point. This equilibrium represents a predator-free state, in which the prey population persists at its carrying level $u^* = 1/\sigma$. The negative eigenvalue indicates the local stability of prey dynamics in the absence of predators, implying that small perturbations in prey density are damped by intrinsic logistic regulation. However, the positive eigenvalue associated with predator direction reveals that this equilibrium is unstable to predator invasion, and even a very small introduction of predators leads to initial population growth. Ecologically, this demonstrates that a prey-dominated environment at equilibrium provides sufficient resources for predator persistence, rendering the predator-free state structurally unstable and unlikely to represent a longterm outcome of system dynamics.

2.2.3 Stability Analysis of the Equilibrium Point E_2

The equilibrium point E_2 is referred to as the interior equilibrium because it lies in the first quadrant of the phase plane, where both state variables are strictly positive, that is, $u^* > 0$ and $v^* > 0$. This equilibrium corresponds to a biologically meaningful coexistence state and is given explicitly by

$$E_2 = (u^*, v^*) = \left(\frac{\mu}{\rho-\mu}, \frac{\rho^2 - \rho\mu(1+\sigma)}{(\rho-\mu)^2}\right),$$

which exists if the conditions $\rho > \mu$ and $\rho > \mu(1+\sigma)$ are satisfied. These inequalities ensure the feasibility of equilibrium and guarantee that both the prey and predator populations persist at positive levels.

For analytical convenience, the following relations are introduce

$$\begin{aligned} 1 + u^* &= \frac{\rho}{\rho-\mu}, \quad \frac{v^*}{(1+u^*)^2} = \frac{\rho - \mu(1+\sigma)}{\rho}, \\ \frac{u^*}{1+u^*} &= \frac{\mu}{\rho}. \end{aligned} \tag{6}$$

Substituting the equilibrium point E_2 into the Jacobian matrix defined in (5), and using the identities in (6), the Jacobian matrix evaluated at E_2 is obtained as

$$J_{E_2} = \begin{bmatrix} \frac{\mu(\mu\sigma + \rho\sigma + \mu - \rho)}{\rho(\rho-\mu)} & -\frac{\mu}{\rho} \\ \mu\sigma + (\rho - \mu) & 0 \end{bmatrix}.$$

The corresponding characteristic equation is

$$-\lambda\left(\frac{\mu(\mu\sigma + \rho\sigma + \mu - \rho)}{\rho(\rho-\mu)} - \lambda\right) + \frac{\mu}{\rho}\left(\mu\sigma + (\rho - \mu)\right) = 0,$$

which can be rewritten in the standard quadratic form

$$\lambda^2 - p_0\lambda + q_0 = 0, \tag{7}$$

where

$$p_0 = \frac{\mu(\mu\sigma + \rho\sigma + \mu - \rho)}{\rho(\rho-\mu)}, \quad q_0 = \frac{\mu}{\rho}\left(\mu\sigma + (\rho - \mu)\right),$$

and the discriminant is

$$\Delta_0 = p_0^2 - 4q_0.$$

Based on the signs of p_0 and Δ_0, the local stability of equilibrium point E_2 can be classified as follows.

a. The quilibrium point E_2 is asymptotically stable if $p_0 < 0$ and $\Delta_0 > 0$, and unstable if $p_0 > 0$.
b. Equilibrium point E_2 is a stable spiral if $p_0 < 0$ and $\Delta_0 < 0$; otherwise, it is an unstable spiral if $p_0 > 0$.
c. The equilibrium point E_2 is neutrally stable when $p_0 = 0$ and $\Delta_0 < 0$.
d. Equilibrium point E_2 cannot be a saddle point because the determinant of the Jacobian matrix at E_2 is strictly positive.

From an ecological perspective, the interior equilibrium point E_2 represents a state of coexistence between the prey and predator populations, in which both species survive at positive and finite population densities. The stability characteristics of this equilibrium reflect the resilience of the ecosystem to small perturbations in the steady state. When E_2 is stable, prey-predator interactions are dynamically balanced, indicating the presence of intrinsic regulatory mechanisms that restore population levels following temporary disturbances. In contrast, the instability of E_2 implies that this balance is fragile, such that small perturbations may be amplified into large population oscillations or may even drive the system toward the extinction of one of the species.

Furthermore, the emergence of damped or sustained oscillatory behavior in the neighborhood of E_2 highlights that prey-predator dynamics are not necessarily static, but may exhibit periodic fluctuations arising from nonlinear trophic interactions. Consequently, the stability properties of the interior equilibrium emphasize the critical role of key biological parameters, such as the intrinsic growth rate of the prey, efficiency of predation, and mortality rate of the predator, in determining whether the ecosystem can sustain long-term coexistence or evolve toward unstable and more complex population dynamics.

2.3 Model with Harvesting

Harvesting activities are activated when the population densities exceed their prescribed threshold levels. Specifically, harvesting of the prey population occurs when $x > T$, and harvesting of the predator population occurs when $y > R$. Under these conditions, the harvesting functions take the forms:

$$H(x) = \frac{p(x-T)}{p+(x-T)}, \quad H(y) = \frac{q(y-R)}{q+(y-R)}.$$

Substituting these harvesting functions into system (1) yields the predator-prey model with threshold harvesting:

$$\begin{aligned} \frac{dx}{dt} &= rx\left(1-\frac{x}{K}\right) - \frac{nxy}{a+x} - \frac{p(x-T)}{p+(x-T)}, \\ \frac{dy}{dt} &= \frac{mnxy}{a+x} - dy - \frac{q(y-R)}{q+(y-R)}. \end{aligned} \tag{8}$$

To facilitate analytical treatment and reduce the number of independent parameters, system (8) was nondimensionalized. Let

$$\omega = \frac{T}{a}, \qquad \alpha = \frac{p}{ar}, \qquad \beta = \frac{p}{a},$$
$$\delta = \frac{nR}{ar}, \qquad \eta = \frac{qn}{ar^2}, \qquad \gamma = \frac{qn}{ar},$$

together with dimensionless variables $u(\tau) = x/a$, $v(\tau) = ny/ar$, and $\tau = rt$. Substituting these transformations into system (8) leads to the following non-dimensional model:

$$\begin{aligned} \frac{du}{d\tau} &= u(1-\sigma u) - \frac{uv}{1+u} - \frac{\alpha(u-\omega)}{\beta+(u-\omega)}, \\ \frac{dv}{d\tau} &= \frac{\rho uv}{1+u} - \mu v - \frac{\eta(v-\delta)}{\gamma+(v-\delta)}, \end{aligned} \tag{9}$$

where ω, δ, η are positive constants and the biologically relevant region is restricted to $u > \omega$ and $v > \delta$.

Let $N(u, v)$ denote the vector field associated with system (9). The Jacobian matrix evaluated at an arbitrary equilibrium point $N(u^*, v^*)$ is given by:

$$J_{N_{(u^*,v^*)}} = \begin{bmatrix} N_1 & N_2 \\ N_3 & N_4 \end{bmatrix}$$

where:

$$N_1 = 1 - 2\sigma u^* - \frac{v^*}{(1+u^*)^2} - \frac{\alpha\beta}{(\beta+(u^*-\omega))^2},$$
$$\mathrm{N}_2 = -\frac{u^*}{1+u^*}, \qquad N_3 = \frac{\rho v^*}{(1+u^*)^2},$$
$$N_4 = \frac{\rho u^*}{1+u^*} - \mu - \frac{\eta\gamma}{(\gamma+(v^*-\delta))^2}.$$

2.3.1 Existence of Equilibrium Points

The existence of the equilibrium point (9) are determined by solving $du/d\tau = dv/d\tau = 0$.

a. Boundary equilibrium on the u-axis

Setting $u = 0$, reduces the second equation of system (9)

$$-\mu v - \frac{\eta(v-\delta)}{\gamma+(v-\delta)} = 0.$$

After simplification, this equation leads to the quadratic form

$$\mu v^2 + (\mu\gamma - \mu\delta + \eta)v - \eta\delta = 0,$$

Let

$$A = \mu, \qquad B = \mu\gamma - \mu\delta + \eta, \quad C = \eta\delta.$$

If $B \geq 0$, exactly one positive solution exists, given by

$$v^* = \frac{-B \pm \sqrt{B^2+4AC}}{2A}.$$

If $B < 0$, all solutions are nonpositive and biologically irrelevant. Hence, a unique biologically feasible boundary equilibrium point is obtained:

$$N_0 = \left(0, \frac{-B+\sqrt{B^2+4AC}}{2A}\right).$$

b. Boundary equilibrium on the v-axis

Setting $u = 0$, the first equation of system (9) becomes

$$u(1-\sigma u) - \frac{\alpha(u-\omega)}{\beta+(u-\omega)} = 0.$$

After algebraic manipulation, this yields the cubic equation

$$\sigma u^3 + (\beta\sigma - \omega\sigma - 1)u^2 + (\omega - \beta - \alpha)u + \omega\alpha = 0$$

Dividing by σ and defining

$$\hat{p} = \frac{\beta\sigma-\omega\sigma-1}{\sigma}, \quad \hat{q} = \frac{\omega-\beta-\alpha}{\sigma}, \quad \text{and} \quad \hat{r} = \frac{\omega\alpha}{\sigma},$$

the equation can be written as

$$u^3 + \hat{p}u^2 + \hat{q}u + \hat{r} = 0 \tag{10}$$

Using Cardano's transformation $u = \tilde{x} - \hat{p}/3$, equation (10) is reduced to the depressed cubic

$$\tilde{x}^3 + \hat{a}\tilde{x} + \hat{b} = 0, \tag{11}$$

where $\hat{a}$ and $\hat{b}$ are appropriately defined constants. Let

$$\hat{n} = \left(\frac{\hat{a}}{3}\right)^3 + \left(\frac{\hat{b}}{2}\right)^2,$$

denotes the discriminant of equation (11). Then, (i) if $\hat{n} > 0$, there is one real root and two complex conjugate roots; (ii) if $\hat{n} = 0$, all roots are real, with at least two

equal roots; and (iii) if $\hat{n} < 0$, all roots are real and distinct. Biologically admissible equilibria correspond to the positive real roots of u.

c. Interior equilibrium point

An interior equilibrium point exists when $u^* > 0$ and $v^* > 0$. Let $N_2 = (u^*, v^*)$, denote the equilibrium of system (9). The equilibrium values satisfy the following equation.

$$u^* = \frac{\mu v^*(\gamma+(v^*-\delta))+\eta(v^*-\delta)}{(\rho-\mu)v^*(\gamma+(v^*-\delta))+\eta(v^*-\delta)},$$

$$v^* = \frac{\big(u^*(1-\sigma u^*)(\beta+(u^*-\omega))-\alpha(u^*-\omega)\big)(1+u^*)}{u^*(\beta+(u^*-\omega))}.$$

This interior equilibrium represents a state of coexistence in which both prey and predator populations persist above their respective harvesting thresholds, reflecting a balance between biological interactions and harvesting pressure.

2.3.2 Stability Analysis of Equilibrium Points

In this section, we investigate the local stability properties of all equilibrium points of the non-dimensional system (9) by analyzing the eigenvalues of the corresponding Jacobian matrices. The qualitative behavior of the system in the neighborhood of each equilibrium point was determined by the signs of these eigenvalues.

a. Stability Analysis of the Boundary Equilibrium Point N_0

The equilibrium point $N_0 = (0, v^*)$ represent the boundary equilibrium located on the v-axis. Substituting N_0 into the Jacobian matrix $J_{N_{(u^*,v^*)}}$, the Jacobian matrix evaluated at N_0 takes the triangular form

$$J_{N_0} = \begin{bmatrix} N_0^1 & 0 \\ N_0^3 & N_0^4 \end{bmatrix},$$

where

$$N_0^1 = 1 - v^* - \frac{\alpha\beta}{(\beta-\omega)^2}, \qquad N_0^3 = \rho v^*,$$

$$N_0^4 = -\mu - \frac{\eta\gamma}{(\gamma+(v^*-\delta))^2}.$$

Since the Jacobian matrix is triangular, its eigenvalues are given directly by

$$\lambda_1 = N_0^1 \quad \text{and} \quad \lambda_2 = N_0^4.$$

It is evident that $N_0^4 < 0$ always holds true because of the positivity of the parameters. Consequently, the local stability of N_0 was determined by the sign of N_0^1. Specifically, (i) if $N_0^1 < 0$, both eigenvalues are negative, and thus, N_0 is locally asymptotically stable. However, if $N_0^1 > 0$, the eigenvalues have opposite signs, and therefore N_0 is a saddle point and unstable. This result implies that the predator-only equilibrium may be stable or unstable, depending on whether the effective growth potential of the prey near extinction is suppressed by harvesting and predation effects.

b. Stability Analysis of the Boundary Equilibrium Point N_1

The equilibrium point $N_1 = (u^*, 0)$ lies on the u-axis, and corresponds to the persistence of the prey population in the absence of predators. The Jacobian matrix evaluated at N_1 is given by:

$$J_{N_1} = \begin{bmatrix} N_1^1 & N_1^2 \\ 0 & N_1^4 \end{bmatrix}$$

where

$$N_1^1 = 1 - 2\sigma u^* - \frac{\alpha\beta}{(\beta+(u^*-\omega))^2},$$

$$N_1^2 = -\frac{u^*}{1+u^*}, \quad N_1^4 = \frac{\rho u^*}{1+u^*} - \mu - \frac{\eta\gamma}{(\gamma-\delta)^2}.$$

The eigenvalues of J_{N_1} are

$$\lambda_1 = N_1^1 \quad \text{and} \quad \lambda_2 = N_1^4,$$

both of which are real. Therefore, the local stability of N_1 can be classified as follows: (i) N_1 is locally asymptotically stable if $N_1^1 < 0$ and $N_1^4 < 0$; (ii) N_1 is unstable if $N_1^1 > 0$ and $N_1^4 > 0$; and (iii) N_1 is a saddle point if N_1^1 and N_1^4 have opposite signs. The stability of N_1 determines whether a prey-only ecosystem remains resilient against predator invasion and harvesting or becomes vulnerable to predator establishment.

c. Stability Analysis of the Interior Equilibrium Point N_2

The equilibrium point $N_2 = (u^*, v^*)$ represents an interior equilibrium, where both prey and predator populations coexist at positive levels. Substituting N_2 into the Jacobian matrix yields.

$$J_{N_2} = \begin{bmatrix} N_2^1 & N_2^2 \\ N_2^3 & N_2^4 \end{bmatrix}$$

where

$$N_2^1 = -2\sigma u^* - \frac{v^*}{(1+u^*)^2} - \frac{\alpha\beta}{(\beta+(u^*-\omega))^2}$$

$$N_2^2 = -\frac{u^*}{1+u^*}, \qquad N_2^3 = \frac{\rho v^*}{(1+u^*)^2},$$

$$N_2^4 = \frac{\rho u^*}{1+u^*} - \mu - \frac{\eta\gamma}{(\gamma+(v^*-\delta))^2}.$$

The characteristic equation with J_{N_2} is

$$\lambda^2 - p_1\lambda + q_1$$

where

$$p_1 = \mathrm{trace}\big(J_{N_2}\big), \quad q_1 = \det\big(J_{N_2}\big),$$

and the discriminant is given by

$$\Delta_1 = p_1^2 - 4q_1.$$

Accordingly, the local stability of N_2 is classified as follows: (i) N_2 is a stable node if $\Delta_1 > 0$ and $p_1 < 0$; (ii) N_2 is a stable spiral if $\Delta_1 < 0$ and $p_1 < 0$; and (iii) N_2 is an unstable spiral if $\Delta_1 < 0$ and $p_1 > 0$. Because determinant $q_1 > 0$ is strictly positive, N_2 cannot be a saddle point. Moreover, a neutrally stable behavior does not occur for biologically admissible parameter values. Thus, interior equilibrium captures the dynamic balance between prey growth, predation pressure, and harvesting intensity, and its stability determines whether long-term coexistence is maintained or disrupted by oscillatory population dynamics.

3 NUMERICAL SIMULATIONS

In this section, the purpose of conducting numerical simulations is to understand the behavior of Model (1), as discussed previously, based on the threshold harvesting functions provided, which can be divided into two forms. The first model is a system without harvesting, where the population densities of prey and predators remain below or equal to the specified thresholds, $x \le T$, $y \le R$, respectively. Here, it is assumed that $H(x) = H(y) = 0$. The second model incorporates harvesting, where the population densities of prey and predators exceed the specified thresholds,

the prey harvesting function is $H(x) = \frac{p(x-T)}{p+(x-T)}$ and the predator harvesting function is $H(y) = \frac{q(y-R)}{q+(y-R)}$.

3.1 Numerical Simulations for the Model Without Harvesting

The simulation results revealed that when intraspecific competition within the populations is minimal, prey populations grow significantly. In contrast, high predator efficiency intensifies the interaction, causing predator populations to grow rapidly and exert substantial pressure on the prey population. Consequently, the prey-predator interaction exhibits strong oscillations, tending toward instability, as illustrated in Figure 1. If predators fail to secure sufficient prey for survival, predator extinction is a likely outcome.

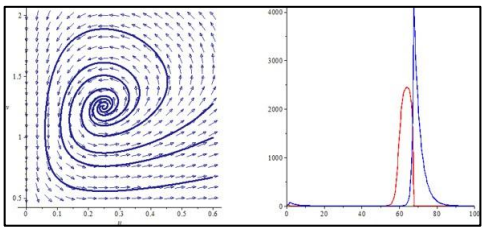

Fig. 1. The stability of the model without harvesting for σ = 0.0004, ρ = 1.5, and μ = 0.3.

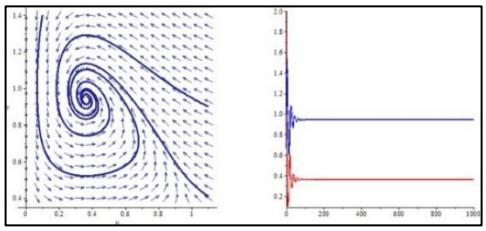

Fig. 2. The stability of the model without harvesting for σ = 0.85, ρ = 0.75, and μ = 0.2.

Furthermore, when the intraspecific competition rate of predators remains constant and their natural mortality rate increases to approach their growth rate, predators are more likely to become extinct. Under such conditions, the prey population stabilizes at its carrying capacity because of the absence of predation pressure. However, if the intraspecific competition rate approaches the carrying capacity of the environment while predator efficiency and natural mortality rates remain constant, prey-predator interactions tend to oscillate toward a stable equilibrium, as shown in Figure 2. This occurs because the high level of competition among prey for resources, mates, or living space slows population growth, even in the absence of predators. This dynamic also causes predator populations to grow more slowly, resulting in subdued and stable population interactions.

3.2 Numerical Simulation with Harvesting

For the model with harvesting, the simulation results indicate that if the harvesting threshold values are close to the interior equilibrium point of the model without harvesting, previously unstable interactions can become stable after harvesting is introduced. Another intriguing observation was that the stability of these interactions was not influenced by the maximum harvesting rate. Consequently, whether the values of p or q are large or small does not affect the stability of the model, as shown in Figure 3. However, if the harvesting thresholds are very low compared with the equilibrium point of the model without harvesting, interactions between the populations that were previously stable could become unstable. In extreme cases, the effects of harvesting threaten the sustainability of both populations.

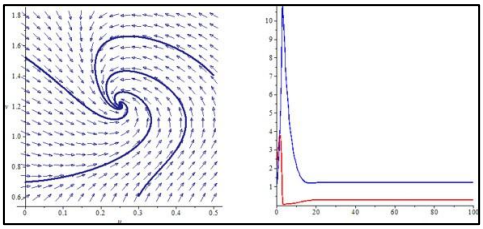

Fig. 3. The stability of the model with harvesting for σ = 0.0004, ρ = 1.5, μ = 0.3, α = 0.42, β = 0.6, ω = 0.24, η = 0.1, δ = 1.2, and γ = 0.7.

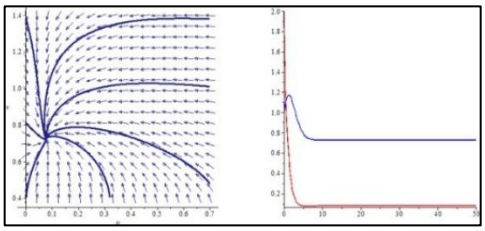

Fig. 4. The stability of the model with harvesting for σ = 0.85, ρ = 0.75, μ = 0.2, α = 0.988, β = 0.82, ω = 0.6, η = 0.255, δ = 0.91, and γ = 0.63.

The simulations also demonstrate that when harvesting is applied to a population that was previously stable, with threshold values set sufficiently high or very close to the interior equilibrium of the model without harvesting, the population interactions remain stable. This stability persists even if the threshold values are reduced to nearly zero, with only minor fluctuations occurring at the onset of harvesting. This phenomenon is illustrated in Figure 4.

4 Conclusions

The study was based on the Lotka-Volterra predator-prey interaction model by incorporating the Holling-Type II functional response and threshold harvesting for both populations. Additionally, the prey population density growth rate in the absence of predators follows the Verhulst model, representing logistic growth toward environmental carrying capacity. Based on the given threshold values, the model is analyzed under two primary scenarios: a non-harvesting model, where the population densities of prey and predators remain below the specified

thresholds, and a harvesting model, where population densities exceed those thresholds.

In the non-harvesting scenario, up to three equilibrium points were identified: trivial, semitrivial, and interior. The analysis indicates that the interior equilibrium point exhibits the most complex dynamics, and its stability is influenced by factors such as the mortality rate of prey, intraspecific competition among prey, and the efficiency of prey-to-predator biomass conversion. Numerical simulations demonstrate that in the absence of harvesting, interactions between the two populations tend to be unstable under certain conditions, particularly when the predator efficiency is very high. In contrast, strong intraspecific competition within a prey population can enhance stability, allowing prey density to approach the carrying capacity of the environment.

In contrast, simulations under the harvesting model show that when harvesting is conducted only when population densities exceed the specified thresholds, previously unstable predator-prey interactions can achieve stability. This stability depends on how closely the threshold value is set relative to the interior equilibrium point of the nonharvesting model. If the threshold value is sufficiently close to the interior equilibrium point, the stability of the interactions can be maintained even under intensive harvesting. However, if the threshold is set too low, it can disrupt the population stability and potentially threaten the sustainability of both species.

By dividing the model into two scenarios based on threshold values, this study provides important information on how well-measured harvesting policies can be implemented to maintain the population balance, ensure species survival, and protect the overall stability of ecosystems.

References

1. A. J. Lotka, Elements of physical biology (Williams and Wilkins Company, Baltimore, 1925).
2. C. S. Chou and A. Friedman, Introduction to mathematical biology: modeling, analysis, and simulations (Springer International Publishing, Switzerland, 2016).
3. D. Tilman, F. Isbell, and M. Cowles, Biodiversity and ecosystem functioning. Annual Review of Ecology, Evolution, and Systematics **45**, (2014). https://doi.org/10.1146/annurev-ecolsys-120213-091917
4. H. Ren, W. Zhao, Dynamics analysis of a stochastic Leslie-Gower predator-prey model with feedback controls. Mathematical Problems in Engineering **2019** (2019). https://doi.org/10.1155/2019/8631272
5. J. Alebraheem, Dynamics of a predator-prey model with the effect of oscillation of immigration of the prey. Multidisciplinary Digital Publishing Institute **13**, (2021). https://doi.org/10.3390/d13010023
6. P. H. Leslie, J. C. Gower, The properties of a stochastic model for the predator-prey type of interaction between two species. Biometrika **47**, (1960). https://doi.org/10.1093/biomet/47.3-4.219
7. P. Mishra, A. Ponosov, J. Wyller, On the dynamics of predator-prey models with role reversal. Physica D: Nonlinear Phenomena **461**, (2024). https://doi.org/10.1016/j.physd.2024.134100
8. Y. Kuang, H. I. Freedman, Uniqueness of limit cycles in Gause-type models of predator-prey systems. Mathematical Biosciences **88**, (1988). https://doi.org/10.1016/0025-5564(88)90049-1
9. Y. Lu, S. Liu, Threshold dynamics of a predator-prey model with age-structured prey. Advances in Difference Equations **2018:164**, (2018). https://doi.org/10.1186/s13662-018-1614-y
10. S. Toaha, The effect of harvesting with threshold on the dynamics of prey predator model. Journal of Physics: Conference Series **1341**, (2019). https://doi:10.1088/1742-6596/1341/6/062021
11. V. Volterra, Fluctuations in the abundance of a species considered mathematically. Nature **118**, (1926). https://doi:10.1038/118558a0